

## Simulation of the time evolution of the Wigner function with a first-principles Monte Carlo method

M. S. Torres, Jr.,\* G. Tosi, and J. M. A. Figueiredo†

*Departamento de Física, Universidade Federal de Minas Gerais, P.O. Box 702, Belo Horizonte, MG, Brazil 30123-970*

(Received 8 April 2009; published 4 September 2009)

The implementation of Monte Carlo methods acting in the quantum phase space is hindered by the fact that quantum phase-space information is available only through quasiprobability densities. In this work, we present a first-principles Monte Carlo method employing a hidden variables representation. This allows the full quantum time evolution of an arbitrary initial quantum state to be calculated by a classical Monte Carlo algorithm, even for systems subjected to time-dependent potentials. Guidelines for implementing a practical algorithm are presented.

DOI: [10.1103/PhysRevE.80.036701](https://doi.org/10.1103/PhysRevE.80.036701)

PACS number(s): 02.70.Ss, 02.50.Ga, 05.10.Ln, 02.50.Ey

### I. INTRODUCTION

The Wigner function is the quantum formulation of the classical phase-space description, being equivalent to the density matrix. It contains information about a particle's position and momentum variables, albeit in a form which is not easy to interpret classically because it is not positive semidefinite. This property prevents the Wigner function from being used as a true phase-space probability density. In fact, it is claimed that the existence of these negative regions of the Wigner function indicate the presence of purely non-classical, quantum phenomena [1].

In the last couple of decades, the Wigner function has been used to study an increasing number of physical systems; of great interest is the fact that, unlike the quantum wave function, there are techniques able to measure the Wigner function of the electromagnetic field, such as optical homodyne tomography [2–4].

This way, it is natural to develop methods of efficient calculation of the Wigner function and its time evolution. One practical possibility is the extension of Monte Carlo techniques to the quantum phase space, which is not trivial because the Wigner function is not a true probability density. While there are many quantum Monte Carlo algorithms for the wave function or density matrix [5–11], there are few such algorithms for the Wigner function [12]. Quantum Monte Carlo methods, whether applied to amplitudes or to phase-space calculations, fall into two basic categories: (1) numerically solving the imaginary time Schrödinger equation using Monte Carlo integration techniques to obtain the ground state wave function (or, in some cases, the density matrix) [5–11] and (2) simulating a random walk of a system of “particles” under a quantum force (usually obtained from an approximation of the Wigner transport equation) to evolve an initial configuration of these “particles” to obtain a Wigner function at a later time [12,13]. In [12], the negativity of the Wigner function forces the use of a number of simulated “particles” much greater than number of actual particles in the real physical system, as well as the need to

use a special prescription to generate the initial state. A recent work [14] presents a rigorous derivation of an algorithm capable of approximating the evolution of the Wigner function of a particular class of two-state systems using classical trajectories and state transitions. In all of these cases, the nonpositiveness of the Wigner function limited the choice of the initial state to Gaussian Wigner functions. Thus, the fact that the Wigner function is not positive semidefinite and the fact that the quantum force is nonlocal, have both hindered so far the implementation of a code simulating all aspects of quantum dynamics using solely classical Monte Carlo techniques.

A first-principles Monte Carlo algorithm capable of simulating the time evolution of quantum probabilities of a one-particle system, subjected to arbitrary time-dependent potential, has been proposed by Figueiredo [15]. This algorithm makes use only of a classical noise source and a set of hidden variables. It shows that quantum effects are obtained by a specific renormalization of the time-evolved histograms. In this work, we will present a formal presentation of a hidden variable stochastic field that allows an extension of that algorithm to the quantum phase space. Therefore, not only quantum probabilities but also phase information contained in the quantum amplitude can be obtained through this new algorithm. This means that there is a first-principles classical Monte Carlo method capable of simulating the whole range of quantum phenomena for spinless particles.

### II. TWO LEVEL TRANSITION MATRICES

In this section, the dynamics of a classical two-state system is shortly presented. Then it will be shown how it can be used to properly describe the dynamics of quasiprobability densities. This enables the construction of a classical Monte Carlo algorithm which could be used to simulate the time evolution of a Wigner function. This two-state system defines a kind of hidden variable acting on a probability space from which quasiprobability values can be restored using a simple algorithm.

Consider the binary random variable  $\alpha$  and its associated probability distribution  $P(t)=[p_0(t) p_1(t)]^T$ , where normalization demands  $p_0(t)+p_1(t)=1$  and, as required of any classical probability model,  $p_0$  and  $p_1$  are positive real numbers. We

\*marzojr@fisica.ufmg.br

†josef@fisica.ufmg.br

will assume that there are no memory effects, so that its time evolution obeys a linear equation of the form

$$\frac{dP(t)}{dt} = \begin{pmatrix} c(t) & b(t) \\ a(t) & d(t) \end{pmatrix} P(t) \equiv r(t)P(t) \quad (1)$$

where the real numbers  $a(t)$ ,  $b(t)$ ,  $c(t)$ , and  $d(t)$  are the transition rates. The solution of this system can be put in the form

$$P(t) = M(t, t_0)P(t_0). \quad (2)$$

Here, the matrix  $M(t)$  is the cumulative transition matrix for  $P$  in the  $(t_0, t)$  interval. Its off-diagonal elements describe the probabilities of changes in the states of  $\alpha$  and the diagonal ones gives the probability of  $\alpha$  staying in the same state. Thus,  $M$  is positive semidefinite, and each of its columns must sum to one. This condition also ensures the normalization of  $P(t)$  at later times. Hence it has the general form

$$M(t, t_0) = \begin{pmatrix} 1 - A(t, t_0) & B(t, t_0) \\ A(t, t_0) & 1 - B(t, t_0) \end{pmatrix}. \quad (3)$$

Note that, while the general form of the cumulative transition matrix is easily obtained, the cumulative transition probabilities  $A(t, t_0)$  and  $B(t, t_0)$  do not have a simple relationship to the matrix  $r(t)$  except in some simple cases (such as the case of time-independent transition probabilities); however, the exact forms of those coefficients are not needed for the formalism we present here. With these considerations in mind, it follows from the listed properties of  $M$  [Eqs. (2) and (3)]

$$\begin{pmatrix} W(t) + v \\ 1 - W(t) - v \end{pmatrix} = \begin{pmatrix} [1 - A(t, t_0) - B(t, t_0)]W(t_0) + [1 - A(t, t_0) - B(t, t_0)]v + B(t, t_0) \\ 1 - [1 - A(t, t_0) - B(t, t_0)]W(t_0) + [1 - A(t, t_0) - B(t, t_0)]v + B(t, t_0) \end{pmatrix}$$

and both sides of this expression can be equated. In view of  $W(t) = K(t, t_0)W(t_0)$  this procedure leads to an expression for the transition matrix  $M(t, t_0)$  whose elements can be expressed in terms of  $v$  and  $K$  as

$$A(t, t_0) = (1 - v)[1 - K(t, t_0)],$$

$$B(t, t_0) = v[1 - K(t, t_0)].$$

More specifically we get  $M$  in the form

$$M(t, t_0) = \begin{pmatrix} 1 - (1 - v)[1 - K(t, t_0)] & v[1 - K(t, t_0)] \\ (1 - v)[1 - K(t, t_0)] & 1 - v[1 - K(t, t_0)] \end{pmatrix} \quad (6)$$

which allows an immediate treatment of the evolution of  $P$  using standard classical tools. The time invariance of  $v$  allows an immediate recovery of  $W(t)$  simply given by  $P_0(t) - v$ . This last step represents a renormalization of the histogram generated by  $P$  and has no ‘‘classical’’ analog. Thus,

that a (classical) Monte Carlo code can readily be written simulating the time evolution of  $\alpha$ .

Now we will show how to make use of this system to describe the time evolution of quasiprobabilities. In the next section we extend our reasoning to the more general case of random fields and show how it can be applied to the simulation of quantum dynamics. In this sense consider a quasiprobability, that is a real-valued function  $W(t)$  with a lower bound  $-v$ , such that  $W(t) \geq -v$  for all  $t$ . Moreover, assume  $|W(t)| \leq 1$  and obeys an equation of the form

$$\frac{dW(t)}{dt} = k(t)W(t). \quad (4)$$

Solutions for this equation can always be put in the form  $W(t) = K(t, t_0)W(t_0)$ . By use of an appropriate definition of a  $W$ -dependant two-level probability vector, we now show how to define a formal stochastic process whose evolution embraces all aspects of the evolution of  $W$  itself thus allowing that well established techniques designed for classical Monte Carlo codes be used in the simulation of  $W$  too. This goal is got first by defining a binary stochastic process having state probabilities given by

$$P(t) = \begin{pmatrix} W(t) + v \\ 1 - W(t) - v \end{pmatrix}. \quad (5)$$

The time evolution of  $P$  must match both  $K(t, t_0)$  and Eq. (1), while preserving the time invariance of  $v$ , necessary to give consistency to this definition. Then, using Eqs. (1) and (3) we get the equivalence

using this formalism, it is possible to define an extended probability space (EPS) describing a hidden variable  $\alpha$  and its associated probability vector from which the dynamics of the real number  $W$  can be readily obtained.

### III. FORMAL HIDDEN-VARIABLE FIELD

Our main purpose, in this section, is to show how is possible to overcome the quasiprobability issues that arise when trying to simulate quantum phase space. A brief summary of its properties are listed in the Appendix. There a path integral in phase space describing its time evolution is also presented.

For a system of  $n$  particles subject to a potential  $V(\mathbf{x}, t)$ , the Wigner function obeys the equation

$$\frac{\partial f(z, t)}{\partial t} + m^{-1} \mathbf{p} \cdot \nabla_x f(z, t) - \frac{2}{\hbar} \sin \left\{ \frac{\hbar}{2} \nabla_x^V \cdot \nabla_p^f \right\} V(\mathbf{x}, t) f(z, t) = 0. \quad (7)$$

Here,  $\nabla_x^V$  acts only on the potential  $V(\mathbf{x}, t)$  and  $\nabla_p^f$  acts only on the Wigner function  $f(z, t)$ . Variable  $z$  comprises the

whole phase-space variables. Defining the operator  $\hat{W}(z, t) \equiv m^{-1} \mathbf{p} \cdot \nabla_x - \frac{\hbar}{2} \sin\{\frac{\hbar}{2} \nabla_x^V \cdot \nabla_p\} V(\mathbf{x}, t)$  leads to  $\frac{\partial f(z, t)}{\partial t} + \hat{W}(z, t) f(z, t) = 0$ , which has the same form of Eq. (4) for each value of  $z$ . Its solution is the Marinov path integral shown in the Appendix [Eq. (A5)]. The short-time evolution kernel  $K(z, t; z', t')$  of the Wigner function between two neighboring time slices  $t'$  and  $t = t' + \varepsilon$ , as presented in the Appendix, is given by

$$\begin{aligned} K(z, t; z', t') &= \left( \frac{1}{2\pi\hbar} \right)^{3n} \delta^{3n}(\mathbf{x}' + m^{-1} \varepsilon \mathbf{p} - \mathbf{x}) \\ &\times \int \delta^{3n}(\mathbf{p} - \mathbf{p}' + \varepsilon \nabla V(\mathbf{x}, t) + \mathbf{Q}) \\ &\times \exp\left\{ -\frac{i}{\hbar} [\mathbf{Q} \cdot \mathbf{s} + \varepsilon g(\mathbf{x}, \mathbf{s}, t)] \right\} d^{3n} s d^{3n} Q \end{aligned} \quad (8)$$

where  $g(\mathbf{x}, \mathbf{s}, t) = V(\mathbf{x} - \frac{1}{2}\mathbf{s}, t) - V(\mathbf{x} + \frac{1}{2}\mathbf{s}, t) + \mathbf{s} \cdot \nabla V(\mathbf{x}, t)$ . Using this kernel, the Wigner function at a later time  $t_{n+1}$  can be obtained from the initial time by a path integral

$$f(z_{n+1}, t_{n+1}) = \int \prod_{j=0}^n K(z_{j+1}, t_{j+1}; z_j, t_j) f(z_0, t_0) d^{6n} z_j. \quad (9)$$

It is clear from this equation that the Wigner function has the Markovian property.

The two delta functions in Eq. (8) effectively make the dynamical variables  $z = (\mathbf{x}, \mathbf{p})$  to evolve according to the following Langevin-like equations

$$\mathbf{x} - \mathbf{x}' = m^{-1} \varepsilon \mathbf{p}, \quad (10a)$$

$$\mathbf{p} - \mathbf{p}' = -\varepsilon \nabla V(\mathbf{x}, t) - \mathbf{Q}, \quad (10b)$$

where  $Q$  plays the role of a noise source. These equations define a path in phase space, where each path has a pseudo-weight given by

$$Wk(\mathbf{x}, \mathbf{Q}, t) = \left( \frac{1}{2\pi\hbar} \right)^{3n} \int \exp\left\{ -\frac{i}{\hbar} [\mathbf{Q} \cdot \mathbf{s} + \varepsilon g(\mathbf{x}, \mathbf{s}, t)] \right\} d^{3n} s. \quad (11)$$

In general, neither the Wigner function nor this pseudo-weight is positive semidefinite; this prevents the use of standard classical Monte Carlo methods to calculate its time evolution. In what follows we show how to use the EPS to define a formal stochastic process based on the Marinov kernel and capable of describing the time evolution of the Wigner function.

Using the boundedness property of the Wigner function, it is always possible to find a pair of uniformly bounded, positive semidefinite functions  $P(z, t)$  and  $\rho(z, t)$  and a constant  $0 \leq \nu \leq 1$ , such that

$$f(z, t) = \rho(z, t) [P(z, t) - \nu] \quad (12)$$

and by an appropriate choice of  $\nu$  and  $\rho$  we can set  $0 \leq P(z, t) \leq 1$ . The Marinov integral then becomes

$$f(z, t) = \int \rho(z', t') K(z, t; z', t') [P(z', t') - \nu] d^{6n} z'. \quad (13)$$

Since we are working in phase space, we need to define a two-state Markov field in order to proceed in an analogous way to section II. For this reason, we now define the probability density vector  $\Pi(z, t) \equiv \rho(z, t) \begin{pmatrix} P(z, t) \\ 1 - P(z, t) \end{pmatrix}$ , which is the generalization to phase space of vector  $P(t)$  defined in Eq. (5) for normalized  $\rho(z, t)$ ; in what follows, we obtain an equation governing the time evolution of vector  $\Pi(z, t)$ . In order to proceed, we must first obtain a matrix analogous matrix to Eq. (6); it must be a matrix density, which we define as

$$\begin{aligned} M &\equiv \begin{pmatrix} \gamma - (\gamma - K)(1 - \nu) & (\gamma - K)\nu \\ (\gamma - K)(1 - \nu) & \gamma - (\gamma - K)\nu \end{pmatrix} \\ &= K + \begin{pmatrix} (\gamma - K)\nu & (\gamma - K)\nu \\ (\gamma - K)(1 - \nu) & (\gamma - K)(1 - \nu) \end{pmatrix}. \end{aligned} \quad (14)$$

Here,  $\gamma(z, t; z', t')$  is a positive semidefinite integrable function chosen so that all elements of matrix  $M$  are positive semidefinite; its primary role is to ensure convergence of path integrals that will appear as a consequence of the Marinov integrals. As we will see below, in an actual algorithm, which must always operate on a finite region of phase space, both  $\gamma$  and  $\rho$  can be taken to be constants; in this case, the formalism becomes much more similar to the analogous case from Sec. II. From definition (14), it follows that

$$M \begin{pmatrix} q \\ -q \end{pmatrix} = K \begin{pmatrix} q \\ -q \end{pmatrix},$$

$$M \begin{pmatrix} \nu \\ 1 - \nu \end{pmatrix} = \gamma \begin{pmatrix} \nu \\ 1 - \nu \end{pmatrix},$$

for all functions  $q$ . Making use of these identities and Eqs. (13) and (14), we find that the time evolution of the vector  $\begin{pmatrix} f \\ -f \end{pmatrix}$  from time  $t'$  to time  $t$  is given by

$$\begin{pmatrix} f(z, t) \\ -f(z, t) \end{pmatrix} = \int \rho' \left[ M(z, t; z', t') \begin{pmatrix} P' \\ 1 - P' \end{pmatrix} - \gamma \begin{pmatrix} \nu \\ 1 - \nu \end{pmatrix} \right] d^{6n} z'. \quad (15)$$

Defining  $\rho \equiv \int \rho' \gamma d^{2n} z' \geq 0$ , this equation becomes

$$\Pi \equiv \rho \begin{pmatrix} P \\ 1 - P \end{pmatrix} = \int M \rho' \begin{pmatrix} P' \\ 1 - P' \end{pmatrix} d^{6n} z' \equiv \int M \Pi' d^{6n} z'. \quad (16)$$

With the restrictions we made for  $\gamma$ ,  $\rho$ , and  $\nu$ , all elements of matrix  $M$  are positive semidefinite; hence,  $P$  will also be positive semidefinite since  $P'$  is; the same also holds for  $1 - P$ . This result is similar to the one obtained earlier [15] for the quantum probability density, and defines a time-dependent two-state system with real probabilities. However, unlike the former formalism, this two-state system has the Markovian property since the Wigner evolution kernel [Eq. (A4)] does; this has the advantage of allowing data generated

TABLE I. Values of the constants used in the simulation of the Gaussian potential well. In this table,  $m$  is the simulated particle's mass,  $V_0$  and  $\sigma$  are the potential's maximum value and half-width [Eq. (22)],  $\beta$  is the half-width of the first element of the Gaussian nonorthogonal basis [Eq. (23)],  $\varepsilon$  is the width of the time slice used, and  $x_{\max}$  and  $p_{\max}$  are half the width of the phase-space box used.

$\hbar = m = V_0 = \beta = 1$
$x_{\max} = 20$
$\sigma = 10$
$\varepsilon = 0.1$
$p_{\max} = \varepsilon x_{\max}$

by the algorithm to be used as the initial conditions of new simulations.

Recursive application of Eq. (16) leads to a chained Markov process defined by

$$\rho(z_{l+1}, t_{l+1}) \begin{pmatrix} P(z_{l+1}, t_{l+1}) \\ 1 - P(z_{l+1}, t_{l+1}) \end{pmatrix} = \int \prod_{n=0}^l M(z_{l+1}, t_{l+1}; z_l, t_l) \rho(z_0, t_0) \times \begin{pmatrix} P(z_0, t_0) \\ 1 - P(z_0, t_0) \end{pmatrix} d^{6n} z_l. \quad (17)$$

As a consequence, we show below that this path integral can be calculated using a classical Monte Carlo code.

In order to obtain an expression more suitable for numerical work, we will select a compact region  $\Omega$  such that, for any desired accuracy  $\delta > 0$ , we have

$$\int_{\Omega} f(z, t) d^{2n} z = 1 - \delta.$$

Region  $\Omega$  will be split into disjoint subregions  $\Omega_j$  such that  $\Omega = \cup_j \Omega_j$ . These definitions allows us to write a discretized version of Eq. (17) in the form

$$\rho(z, t) \begin{pmatrix} P(z, t) \\ 1 - P(z, t) \end{pmatrix} = \sum_j M_j \rho_j' \begin{pmatrix} P_j' \\ 1 - P_j' \end{pmatrix} \Delta \Omega_j, \quad (18)$$

where the subscript  $j$  in  $F$ ,  $M$ ,  $\rho'$ , and  $P'$  indicates the mean value of the function in the subregion  $\Omega_j$ , and  $\Delta \Omega_j$  is the volume of that subregion. Since  $\Omega$  is compact, we can choose  $\gamma_j$  so that  $\gamma_j \Delta \Omega_j = 1$  for all  $j$ , and we can also take  $\rho$  to be a constant. Thus, Eq. (18) takes the following discretized form:

$$\begin{aligned} \Pi &\equiv \begin{pmatrix} P \\ 1 - P \end{pmatrix} \\ &= \frac{1}{Z} \sum_j \begin{pmatrix} 1 - (1 - K_j \Delta \Omega_j)(1 - \nu) & (1 - K_j \Delta \Omega_j) \nu \\ (1 - K_j \Delta \Omega_j)(1 - \nu) & 1 - (1 - K_j \Delta \Omega_j) \nu \end{pmatrix} \\ &\quad \times \begin{pmatrix} P_j' \\ 1 - P_j' \end{pmatrix} \\ &\equiv \frac{1}{Z} \sum_j M_j \Pi_j', \end{aligned} \quad (19)$$

where  $Z = \rho / \rho' = \int \gamma d^{2n} z' = \sum_j \gamma_j \Delta \Omega_j = \sum_j 1$  is the number of subregions in  $\Omega$ . Since matrix  $M$  and vector  $\Pi'$  are both positive semidefinite and since their columns sum to 1, this equation defines a path in a discrete two-level Markov chain given by

$$\Pi(z_{l+1}, t_{l+1})_{path} = \prod_{n=0}^l M(z_{l+1}, t_{l+1}; z_l, t_l) \Pi(z_0, t_0). \quad (20)$$

The total probability  $\Pi$  at the final time is given by the sum of all paths divided by the normalization constant  $Z^{l+1}$ . This is similar to the result we obtained in the previous section: we have defined an extended probability space in which the time evolution of the Wigner function can be recovered from the time evolution of a classical binary random hidden variable field. It must be noticed that this hidden variable field does not directly influence values of observables which depend only on values of the Wigner function.

At time  $t$ , the resulting histogram obtained by Eq. (19) must be inserted in the expression (12), which after a proper renormalization, results in

$$f = \frac{1}{\sum_j (P - \nu)_j} (P - \nu). \quad (21)$$

A practical realization of an algorithm simulating this stochastic process may follow the same guidelines described in [15].

As developed, this method is applicable to an arbitrary number of spinless particles subjected to an arbitrary scalar time-dependent potential. Its greatest advantage, however, is that it allows the use of standard classical Monte Carlo techniques in the study of quantum dynamics. These features allow the method to be applied to the simulation of problems where the Wigner function is already a useful tool, like transport problems in semiconductors [16–18]. Moreover, it can also be used for the study of time-dependent systems such as the interaction of molecules with ultrashort laser pulses [19] or the analysis of time-dependent many-body problems [20]; this can be readily achieved with our formalism by supplying the correct time-dependent potential on each time slice. However, the case of large multidimensional systems shares the same difficulties that standard classical Monte Carlo algorithms have for simulating large multidimensional mechanical systems.

#### IV. RESULTS OF A PRACTICAL IMPLEMENTATION

In order to test the formalism, we wrote a code that simulates a simple one-dimensional system subject to an attractive Gaussian potential given by

$$V(x) = -V_0 \exp\left(-\frac{x^2}{2\sigma^2}\right). \quad (22)$$

This particular system was chosen because it admits approximate eigenstate solutions [21] which were used to check the accuracy of our work. This potential also has the advantage of being bounded, making it more suitable for numerical work. Finally, the fact that it is not harmonic allows us to test

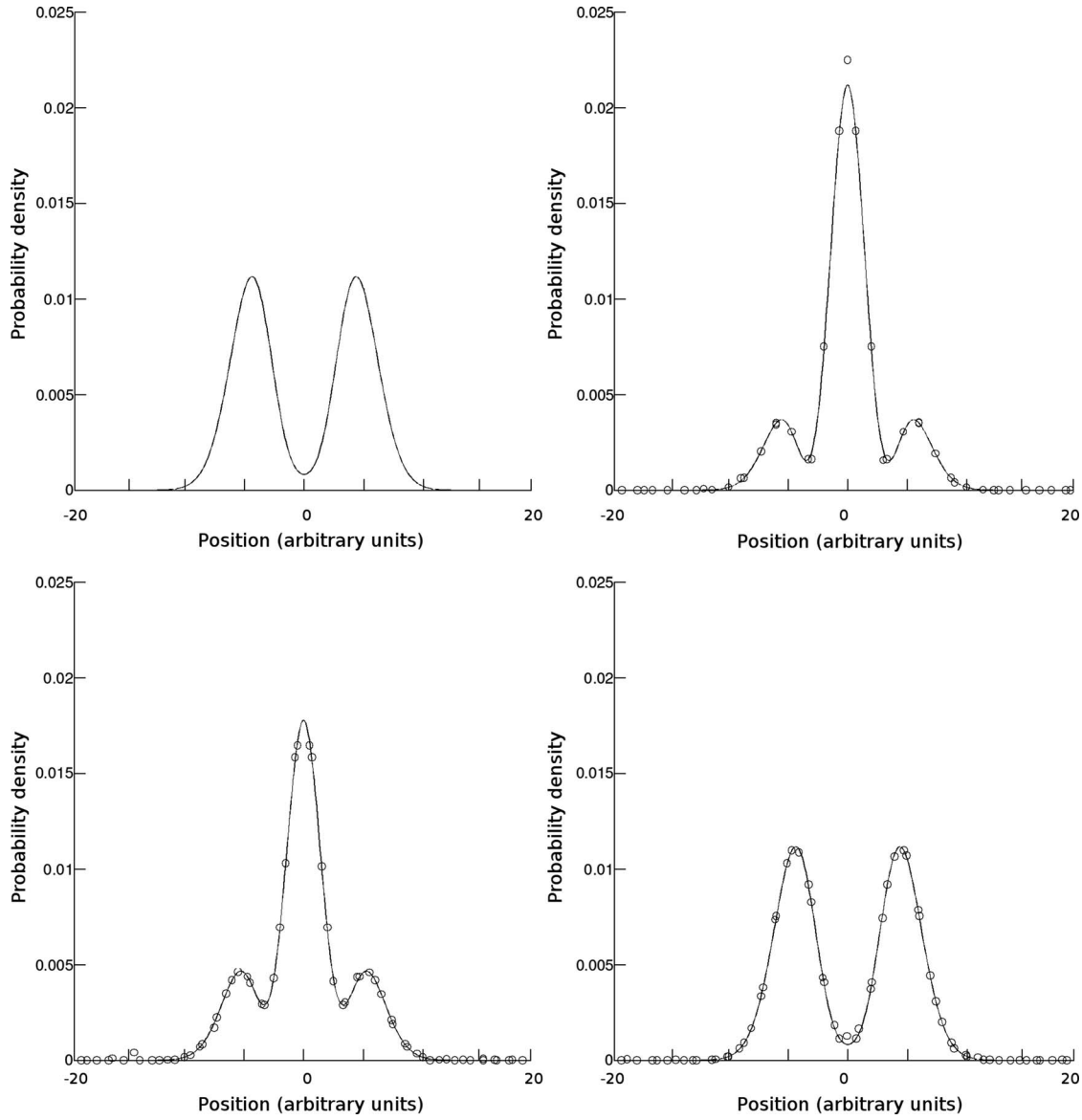


FIG. 1. Comparison of probability densities for Gaussian potential at various time steps. Solid lines are the eigenvalue and eigenvector solutions, while symbols are the numerically integrated algorithm output. The algorithm output shows one out of every ten data points. *Top left*: initial probability density. *Top right*: probability density at instant 123ε. *Bottom left*: probability density at instant 228ε. *Bottom right*: probability density at instant 333ε.

all aspects of our algorithm which, in the harmonic case, is considerably simpler.

The eigenstates associated to this potential can be written by an expansion on a set of nonorthogonal normalized Gaussian wave functions of the form [21],

$$\psi_k(x) = (\sqrt{\pi k \beta^2})^{-1/2} \exp\left(-\frac{x^2}{2k\beta^2}\right). \quad (23)$$

In this basis, they can be written in the form

$$\Psi_\lambda(x, t) = \sum_{k=1}^{\infty} a_{\lambda k} \psi_k(x) \exp\left(-\frac{i}{\hbar} E_\lambda t\right). \quad (24)$$

Coefficients  $a_{\lambda k}$  and energy eigenvalues  $E_\lambda$  are given by the generalized eigenvalue equation

$$\sum_{k=1}^{\infty} (T_{jk} + V_{jk} - E_\lambda B_{jk}) a_{\lambda k} = 0, \quad (25)$$

where  $T_{jk}$  and  $V_{jk}$  are the matrix coefficients of the kinetic and potential terms of the Hamiltonian and

$$B_{jk} = \int \psi_j^*(x) \psi_k(x) dx. \quad (26)$$

Equation (25) is of infinite dimension. With this in mind, we decided to simulate a system in a bound initial state, as such states naturally fit within a compact region of phase space. Moreover, using a bound state allows us to restrict the range of  $k$  to a maximum value  $k=k_{\max}$ , since high values of  $k$  correspond to near uniform Gaussians that do not contribute

TABLE II. Comparison of simulated and numerical results.  $f_S$  is the Wigner function obtained by the simulation, while  $f_C$  is the Wigner function obtained by the approximate eigenstate solution. The instants shown are the same as those presented in Fig. 1.  $C(f_S, f_C)$  is the Pearson correlation coefficient of  $f_S$  and  $f_C$ .

Time	$C(f_S, f_C)$	$\sigma( f_S - f_C )$	$ 1 - \frac{\max(f_S)}{\max(f_C)} $	$ 1 - \frac{\min(f_S)}{\min(f_C)} $
123 $\varepsilon$	0.992	$1.99 \times 10^{-6}$	1.08%	5.30%
228 $\varepsilon$	0.990	$2.18 \times 10^{-6}$	0.29%	0.69%
333 $\varepsilon$	0.986	$2.65 \times 10^{-6}$	1.97%	0.99%

to the normalized wave function. It should be stressed that this is not a limitation of the algorithm itself since the simulation of a nonbounded state could either use different compact regions for each time slice or one large enough to contain the system throughout all time slices.

We numerically solved Eq. (25) using a value of  $k_{\max}=9$ . The initial wave function  $\Phi(x,0)$  was built from the two lowest energy eigenstates,  $\Psi_0(x,0)$  and  $\Psi_1(x,0)$ , using the same weight for both of them. This particular state was chosen because it yields a bound state with interference effects. The wave function at time  $t$  is thus given by

$$\Phi(x,t) = \frac{1}{\sqrt{2}} \left[ \Psi_0(x,0) \exp\left(-\frac{i}{\hbar} E_0 t\right) + \Psi_1(x,0) \exp\left(-\frac{i}{\hbar} E_1 t\right) \right]. \quad (27)$$

This expression can be used to calculate the Wigner function for this system at an arbitrary time.

For the practical realization of the algorithm, we divided the phase-space region into  $401 \times 401$  cells of equal size, centered at the origin. We have ensured that this Wigner function, and its associated probability density, are both normalized to within 1%. The parameters used in the present simulation are shown in Table I.

By means of the code we wrote, the zero-time Wigner function was evolved until time slice 333, each one having width  $\varepsilon$ ; this particular end time is slightly over (by about 0.04%) one full period of the system's oscillation. To integrate the Langevin equation, we have used an embedded Runge-Kutta-Fehlberg (4,5) method provided by the GNU Scientific Library [22]. It should be noted that no effort was spent in code optimization or efficiency since the primary focus of our work was to prove that such a code is possible. The Wigner function at intermediate times can be obtained from the histogram data of the appropriate time slice. Figure 1 displays a comparison between the simulated and calculated quantum probability densities at various times, each obtained by numerical integration of the corresponding Wigner function.

Table II shows the Pearson correlation coefficient of the simulated ( $f_S$ ) and calculated ( $f_C$ ) Wigner functions, the standard deviation of the difference  $f_S - f_C$  and the relative difference of maxima and minima of the Wigner functions, for the same time steps as presented in Fig. 1. We ran a total of  $1.0 \times 10^8$  histories for the full simulation; this corresponds to an average of about 622 histories per phase-space cell. We

also see from Table II that the standard deviation error between the simulated and calculated Wigner function is estimated to be  $9 \times 10^{-5}\%$  per time slice. As expected, there is a degradation over time of the error band of the simulation, but all errors are consistent with the initial error of about 1% of the normalization in the working region and the approximation we used for the evolution kernel. A simple extrapolation from our algorithm indicates that, for similar accuracy, the number of histories would grow approximately quadratically with the number of time slices; this is a consequence of the Markovian nature of the presented formalism. Similarly, and in analogy to the classical case, we would expect that the number of histories, for a given accuracy, increases exponentially with the dimension of phase space. However, the same techniques used for the classical case could be applied here to improve efficiency.

## V. CONCLUSION

We have reviewed and extended the formalism from [15] to simulate the time evolution of an arbitrary initial Wigner function forward by a finite amount of time. It is an alternative to other methods that are able to propagate an initial wave function or density matrix. Moreover, since the algorithm simulates quantum mechanics in phase space, expectation values of physical observables can be obtained by direct numerical integration of classical phase-space observables weighted by the Wigner function.

The sample given in the present work shows that the first-principles Monte Carlo code we have developed admits a practical implementation. Also, given that the formalism we presented makes use only of true probability densities, proven classical Monte Carlo techniques can be used to develop algorithms able to simulate a more complex class of physical problems where quantum effects are important. Comparison of our simulation results with theoretical calculations indicates that the simulation error increases monotonically with time. However, our simulations indicate that this error can be made arbitrarily small, for any given time, with a large enough number of histories. Our results show that the code we developed was able to correctly describe the quantum evolution. It gives complete information about the quantum state of the system with a high temporal resolution.

As touched in [15], the existence of a classical Monte Carlo method capable of fully describing all aspects of quantum dynamics raises questions concerning possible phenomena of stochastic nature underlying quantum physics. It must be noted, however, that the operation of adding a reference value to the Wigner function in order to obtain a probability density, while mathematically and algorithmically straightforward, does not have an easy interpretation in terms of the classical statistical theory. Thus, no physical meaning can be easily assigned to this rule; hence, it has a purely operational character. However, this should not be considered as a weakness of the formalism since the wave function has a similar status in the Copenhagen interpretation.

## ACKNOWLEDGMENT

This work was partially funded by Brazilian agency CNPq.

## APPENDIX: THE WIGNER FUNCTION

In this section we shortly list some properties of the Wigner function. It has several interesting properties (see, e.g., [23]), some of which make it an ideal candidate for use in numerical simulations. It is a particular phase-space representation of the density matrix, defined as the image of the density matrix by the inverse Weyl map given by

$$f(\mathbf{x}, \mathbf{p}, t) = \left( \frac{1}{2\pi\hbar} \right)^{3n} \int \left\langle \mathbf{x} + \frac{1}{2}\mathbf{y} \left| \hat{\rho} \right| \mathbf{x} - \frac{1}{2}\mathbf{y} \right\rangle e^{-i\mathbf{p}\cdot\mathbf{y}/\hbar} d^{3n}y. \quad (\text{A1})$$

The first important property of the Wigner function we are interested in is that it contains the same amount of information as the density matrix of the system [24]. However, unlike the classical case it cannot be properly treated as a probability density because it may assume negative values. In addition, it is uniformly bounded [24],

$$|f(\mathbf{x}, \mathbf{p}, t)| \leq \left( \frac{2}{h} \right)^{3n}. \quad (\text{A2})$$

These bounds are also valid for mixed states since the density matrix for such states can be written as a statistical mixture of pure states [23]. As consequence of Eq. (A2), any integral of the Wigner function in an arbitrary compact region of phase space is bounded; this property is extremely important in the implementation of numerical algorithms based on the Wigner function as it ensures that expectation values of bounded observables are bounded.

Similarly to the quantum amplitudes, time evolution of the Wigner function has the Markovian property; that is, it can be written in the form

$$f(z, t) = \int K(z, t; z', t') f(z', t') d^{6n}z' \quad (\text{A3})$$

[here,  $z=(\mathbf{x}, \mathbf{p})$  and  $d^{6n}z \equiv d^{3n}x d^{3n}p$ ] where  $K(z, t; z', t')$  is the Wigner evolution kernel. Since it will be needed for the development of our formalism, we will present here a derivation of its short-time approximation. Starting with the short-time Feynman kernel for the probability amplitude [26]:

$$\begin{aligned} \psi(\mathbf{x}, t) &= \left[ \frac{\det(m)}{(2\pi i\hbar\varepsilon)^{3n}} \right]^{1/2} \\ &\times \int \exp \left\{ \frac{i}{\hbar} \left[ \frac{(\mathbf{x} - \mathbf{x}') \cdot m(\mathbf{x} - \mathbf{x}')}{\varepsilon} - \varepsilon V(\mathbf{x}, t) \right] \right\} \\ &\times \psi(\mathbf{x}', t') d^{3n}x', \end{aligned}$$

where  $\varepsilon \equiv t - t'$  and  $m$  is the mass matrix, a diagonal  $3n \times 3n$  matrix composed of the masses of each individual par-

ticle, each with a multiplicity equal to 3 (the dimension of the space). Inserting this expression into Eq. (A1), and making use of its inverse,

$$\left\langle \mathbf{x} + \frac{1}{2}\mathbf{y} \left| \hat{\rho} \right| \mathbf{x} - \frac{1}{2}\mathbf{y} \right\rangle = \int f(z, t) e^{i\mathbf{p}\cdot\mathbf{y}/\hbar} d^{3n}p$$

we obtain

$$\begin{aligned} K(z, t; z', t') &= \frac{\det(m)}{[(2\pi\hbar)^2\varepsilon]^{3n}} \int \exp \left\{ \frac{i}{\hbar} \left[ \mathbf{p}' \cdot \boldsymbol{\alpha} - \mathbf{p} \cdot \mathbf{w} \right. \right. \\ &\quad \left. \left. + \frac{(\mathbf{w} - \boldsymbol{\alpha}) \cdot m(\mathbf{x} - \mathbf{x}')}{\varepsilon} \right] \right\} \\ &\times \exp \left\{ \frac{i}{\hbar} \varepsilon \left[ V\left(\mathbf{x} - \frac{1}{2}\boldsymbol{\alpha}, t\right) - V\left(\mathbf{x} + \frac{1}{2}\boldsymbol{\alpha}, t\right) \right] \right\} \\ &\times d^{3n}w d^{3n}\boldsymbol{\alpha}. \end{aligned}$$

Since the exponential in the integrand is linear in the variable  $w$ , its integral can be explicitly performed, yielding a Dirac delta function of the form  $\delta^{3n}[\frac{m}{\varepsilon}(m^{-1}\varepsilon\mathbf{p} + \mathbf{x}' - \mathbf{x})]$ . Inserting this in the above expression, we obtain

$$\begin{aligned} K(z, t; z', t') &= \frac{\det(m)}{(2\pi\hbar\varepsilon)^{3n}} \delta^{3n} \left[ \frac{m}{\varepsilon}(m^{-1}\varepsilon\mathbf{p} + \mathbf{x}' - \mathbf{x}) \right] \\ &\times \int \exp \left\{ -\frac{i}{\hbar} \boldsymbol{\alpha} \cdot \left[ \frac{m(\mathbf{x} - \mathbf{x}')}{\varepsilon} - \mathbf{p}' \right] \right\} \\ &\times \exp \left\{ -\frac{i}{\hbar} \varepsilon \left[ V\left(\mathbf{x} + \frac{1}{2}\boldsymbol{\alpha}, t\right) \right. \right. \\ &\quad \left. \left. - \varepsilon V\left(\mathbf{x} - \frac{1}{2}\boldsymbol{\alpha}, t\right) \right] \right\} d^{3n}\boldsymbol{\alpha} \\ &= \left( \frac{1}{2\pi\hbar} \right)^{3n} \delta^{3n}(\mathbf{x}' + m^{-1}\varepsilon\mathbf{p} - \mathbf{x}) \\ &\times \int \cos \left\{ \frac{\mathbf{p} - \mathbf{p}'}{\hbar} \cdot \mathbf{s} - \frac{\varepsilon}{\hbar} \left[ V\left(\mathbf{x} - \frac{1}{2}\mathbf{s}, t\right) \right. \right. \\ &\quad \left. \left. - V\left(\mathbf{x} + \frac{1}{2}\mathbf{s}, t\right) \right] \right\} d^{3n}s. \quad (\text{A4}) \end{aligned}$$

Using this kernel, the Wigner function at a later time  $t_{n+1}$  can be obtained from the initial time by a path integral

$$f(z_{n+1}, t_{n+1}) = \int \prod_{j=0}^n K(z_{j+1}, t_{j+1}; z_j, t_j) f(z_0, t_0) d^{6n}z_j \quad (\text{A5})$$

in full consistency with the results obtained by Marinov [25]. However, given that both the Wigner function and its kernel can take negative values, neither can be used in classical Monte Carlo codes.

- [1] N. Lütkenhaus and S. M. Barnett, Phys. Rev. A **51**, 3340 (1995).
- [2] K. Vogel and H. Risken, Phys. Rev. A **40**, 2847 (1989).
- [3] G. M. D'Ariano, U. Leonhardt, and H. Paul, Phys. Rev. A **52**, R1801 (1995).
- [4] D. T. Smithey, M. Beck, J. Cooper, M. G. Raymer, and A. Faridani, Phys. Scr. **T48**, 35 (1993).
- [5] J. B. Anderson, J. Chem. Phys. **63**, 1499 (1975).
- [6] D. M. Ceperley, Rev. Mod. Phys. **67**, 279 (1995).
- [7] W. L. McMillan, Phys. Rev. **138**, A442 (1965).
- [8] N. D. Drummond, Z. Radnai, J. R. Trail, M. D. Towler, and R. J. Needs, Phys. Rev. B **69**, 085116 (2004).
- [9] D. Ceperley and G. V. Chester, Phys. Rev. B **16**, 3081 (1977).
- [10] J. F. Corney and P. D. Drummond, Phys. Rev. Lett. **93**, 260401 (2004).
- [11] S. Baroni and S. Moroni, Phys. Rev. Lett. **82**, 4745 (1999).
- [12] L. Shifren, C. Ringhofer, and D. K. Ferry, IEEE Trans. Electron Devices **50**, 769 (2003).
- [13] Yu. E. Lozovik and A. V. Filinov, J. Exp. Theor. Phys. **88**, 1026 (1999).
- [14] C. Lasser, T. Swart, and Stefan Teufel, Commun. Math. Sci. **5**, 789 (2007).
- [15] J. M. A. Figueiredo, Physica A **386**, 167 (2007).
- [16] F. Rossi, C. Jacoboni, and M. Nedjalkov, Semicond. Sci. Technol. **9**, 934 (1994).
- [17] H. Kosina, Int. J. Comput. Eng. Sci. **2**, 100 (2006).
- [18] X. Oriols, J. J. García-García, F. Martín, J. Suñé, J. Mateos, T. González, T. Pardo, and O. Vanbésien, Semicond. Sci. Technol. **14**, 532 (1999).
- [19] I. P. Christov, J. Chem. Phys. **128**, 244106 (2008).
- [20] C. C. Martens, Phys. Rev. A **45**, 6914 (1992).
- [21] C.-Y. Wong, J. Opt. B: Quantum Semiclassical Opt. **5**, S420 (2003).
- [22] GNU Scientific Library, available at <http://www.gnu.org/software/gsl/>
- [23] F. Antonsen, Int. J. Theor. Phys. **37**, 697 (1998).
- [24] G. A. Baker, Jr., Phys. Rev. **109**, 2198 (1958).
- [25] M. S. Marinov, Phys. Lett. A **153**, 5 (1991).
- [26] H. Kleinert, *Path Integrals in Quantum Mechanics, Statistics, Polymer Physics, and Financial Markets* (World Scientific Publishing, Singapore, 2004).